Nanomaterials and Energy

One-dimensional nanostructured materials for solar energy harvesting
Han, Wang and Ho
ice | science

http://dx.doi.org/10.1680/nme.11.00005
Paper 1100005
Received 30/07/2011 Accepted 24/09/2011
Published online 03/10/2011
Keywords: nanomaterials & photovoltaics & nanostructures

ice Institution of Civil Engineers
publishing

One-dimensional nanostructured materials for solar energy harvesting

1 **Ning Han** PhD
Senior Research Associate, Department of Physics and Materials Science, City University of Hong Kong, Hong Kong SAR, China

2 **Fengyun Wang** MPhil
Doctoral Student, Department of Biology and Chemistry, City University of Hong Kong, Hong Kong SAR, China

3 **Johnny C. Ho** PhD
Assistant Professor, Department of Physics and Materials Science, City University of Hong Kong, Hong Kong SAR, China

As the energy demand is rapidly increasing worldwide compared with the supply, there is an urgent need to develop alternative energy-harvesting technologies to sustain the economic growth. Among them, solar energy is one of the most promising sources as it is clean, abundant and renewable. Due to the unique optical and electrical properties, one-dimensional (1D) nanostructured semiconductors are attractive materials for the construction of active energy-harvesting devices. In this review article, applications of 1D nanostructured materials – including photovoltaics, photoelectrochemical cells and solar hydrogen production – in solar energy harvesting are summarised. With the efficiency enhancement and cost reduction, 1D nanostructured solar energy harvesting devices are found to be promising to tackle the future energy issue.

1. Introduction

Currently, our modern society is highly relied on fossil fuels such as coal, crude oil and natural gas for the energy supply that will lead to the quick depletion of natural resources in a foreseeable future. At the same time, when these fuels are combusted for the production of energy, large amounts of greenhouse gases are inevitably emitted and pollute our environment. All these have urged us to explore alternative clean energy sources for sustainable human activities (Service, 2005). In this regard, renewable energy sources such as mechanical (Wang and Song, 2006), heat (Cole, 1983) and solar energies (Crabtree and Lewis, 2007; Lewis, 2007) are being actively investigated. Among all alternatives, solar energy is the most fascinating one as it can provide unmetered amount of energy in a clean way – for example, the energy delivered from the sun to earth in an hour will be equivalent to the current amount of energy the entire world consumes in a year.

Even though the harvesting and storage techniques of solar energy are attractive and promising to tackle the energy shortage and corresponding environmental pollution problems, exploring solar energy in a low-cost and high-efficiency way is not easy because (a) the solar energy density is far lower than any of the fossil energy; (b) sunlight is staggering in different areas (plain or plateau, tropical or polar area) and in different time spans (day or night, sunny or cloudy); (c) the solar energy is difficult to be stored in the form of electricity or heat as compared with fossil fuel that stores energy in chemical bonds (Crabtree and Lewis, 2007). These are the main reasons why solar energy accounts to as little as ~0.015% of the total energy used today (Crabtree and Lewis, 2007).

Basically, solar energy can be harvested in the form of biomass, heat and electricity. Compared with the energy conversion efficiencies into biomass and heat (commonly ~0.3% and 20%; Lewis, 2007), conversion of sunlight directly into electricity has the highest theoretical efficiency and flexibility. Therefore, there is a great potential for us to explore free and clean sunlight in the form of electricity by techniques such as photovoltaics (PVs; Fan and Ho, 2011), photoelectrochemical cells (PECs) and in the form of electricity-storing solar hydrogen. To date, the efficiencies of typical commercial solar cells are ~18% for single-crystal silicon-based PVs, ~11% for titanium dioxide (TiO_2)-based dye-sensitised solar cells (DSSCs) and ~18% for solar hydrogen production (Crabtree and Lewis, 2007; Gratzel, 2001; Van de Krol *et al.*, 2008).

Due to the progress of nanotechnology, nanostructured semiconductor materials, such as silicon nanowires and TiO_2 nanoparticles, have

facilitated the cost reduction in device processing and improvement in energy conversion efficiency. In order to make the solar energy harvesting more competitive compared with the fossil energy, a vast amount of research groups are dealing with the fundamentals as well as applicable researches on nanomaterial-based low-cost and high-efficiency third generation solar cells (Kamat, 2007). One dominant advantage of using nanomaterials for energy harvesting is the reduction in the amount of active materials consumed as compared with the entire wafer required for the bulk silicon-based first generation PVs (Garnett and Yang, 2008; Tsakalakos *et al.*, 2007), thus lowering the materials cost without compromising the efficiency. Furthermore, the facile synthesis of nanomaterials is demonstrated to reduce the processing cost compared with the expensive epitaxial growth of second generation thin-film solar cells (Lewis, 2007). In this context, this article reviews the fundamentals and applications of one-dimensional (1D) nanomaterials (nanowires, nanorods, nanotubes etc.) in the solar energy harvesting. Specifically, the assemblies of nanomaterials in various active device structures in solar cells are addressed, which is appealing as they can reduce the materials and processing cost and simultaneously improve the efficiency due to their unique optical and electronic properties (Ford *et al.*, 2009; Gudiksen *et al.*, 2002; Takei *et al.*, 2010; Yan *et al.*, 2009, 2011).

2. Fundamental properties of one-dimensional nanostructured materials

Generally, harvesting sunlight by solar cells includes two successive procedures: generation of excitons (photogenerated electron and hole pair) induced by photon absorption by semiconductor materials with the proper electronic bandgap and separation of excitons by the built-in electric potential gradient. The preferential use of 1D nanomaterials lies in the fact that they can trap photons more effectively with the proper geometrical configuration in the exciton generation step, and also their physical dimensions are similar to the carrier diffusion length to facilitate the collection of free carriers in the exciton separation step, both of which can lead to a further increase in the energy conversion efficiency (Garnett *et al.*, 2011; Hochbaum and Yang, 2010; Yan *et al.*, 2009).

The efficiency of the current device is mainly limited by the inefficient photon absorption in two aspects: (a) photons with energy lower than the bandgap will not get absorbed while those with higher energy would produce hot carriers and (b) photons would get reflected back by the top surface of the device structure. To overcome this, nanomaterials can be engineered with tunable bandgap by tailoring their physical dimensions, which can enhance the overlap with the solar spectra and thus make the most use of the sunlight (Huynh *et al.*, 2002; Klimov, 2006). On the other hand, it is well known that nanoparticles with a size of <100 nm are transparent to light as the dimension is far smaller than the wavelength of light. Therefore, larger particles up to several micrometres are needed to be mixed to effectively scatter the incident light for complete absorption (Wang *et al.*, 2004; Zhang *et al.*, 2008). Although the axial length of 1D nanomaterials is usually in the scale of hundreds of nanometres to tens of micrometres, they can scatter light effectively like the larger nanoparticles mentioned above (Tan and Wu, 2006; Wang *et al.*, 2004). Experiments show that zinc oxide (ZnO) nanorod arrays can serve as an effective anti-reflection coating in a broadband range of 400–1200 nm (Lee *et al.*, 2008) while similar effect is observed for silicon (Garnett and Yang, 2010; Peng *et al.*, 2005; Tsakalakos *et al.*, 2007), gallium nitride (GaN; Tang *et al.*, 2008) and gallium phosphide (Diedenhofen *et al.*, 2009) nanowire arrays. Especially for nanotubes, the light absorbance is even higher because light would be scattered and absorbed several times once it is trapped in the inner cavity (Zhu *et al.*, 2007). To get a general guideline, Muskens *et al.* (2008) reported that the light reflection, which decreases the photon harvesting, would be suppressed by increasing the ratio of the non-diffusive absorption and diffusive scattering.

Theoretically, Hu and Chen (2007) calculated that the nanowire (NW) array has a higher absorbance in the high frequency (short wavelength) region than their thin-film counterparts, because NW array reflects less amount of light due to the periodic structure. This structure can absorb not only the photons incident directly on it but also the photons scattering among its structure although the absorbance can be tailored by tuning the NW filling factor in the low-frequency region (long wavelength) to get a higher absorbance (Hu and Chen, 2007). Successful 1D nanomaterials for effective photon absorption are the tapered silicon nanowire array reported by Jung *et al.* (2010) and the dual diameter germanium nanopillars demonstrated by Fan *et al.* (2010). As shown in Figure 1, the low filling factor (diameter = 60 nm) nanopillar arrays (Figure 1b; blue curve) have a better light absorbance in the high-frequency region (wavelength = 300–600 nm) whereas the higher filling factor (diameter = 130 nm) nanopillar arrays are better in the low-frequency region (wavelength = 600–900 nm; Figure 1b, green curve). This way, the low and high filling factors can be combined to design nanopillars into a dual-diameter bowling-bottle-like nanopillar array to get a higher absorbance of 99% in the broadband region of 300–900 nm (Figure 1b, red curve). In this design, the small diameter tips would transmit (absorb in the meanwhile, but with little reflection) photons as much as possible to the bottom, where the photons can be absorbed to a maximal extent by the high filling factor large diameter part.

Furthermore, the carrier collection efficiency is determined by the relationship between the recombination time of photogenerated electrons and holes and the collection time of photocarriers from the materials surface to the circuits. To enhance the efficiency, either the recombination time should be extended or the collection time should be controlled. As shown in Figure 2, 1D nanomaterials could serve as an electron expressway in the axial direction, which favours electron collection than the nanoparticles due to the shorter collection time. This is demonstrated in the single-crystalline ZnO that electron collection efficiency is enhanced due to the far shorter collection time than that of polycrystalline ZnO materials (Martinson *et al.*, 2006). Quantitatively, the electron mobility in single-crystalline TiO_2

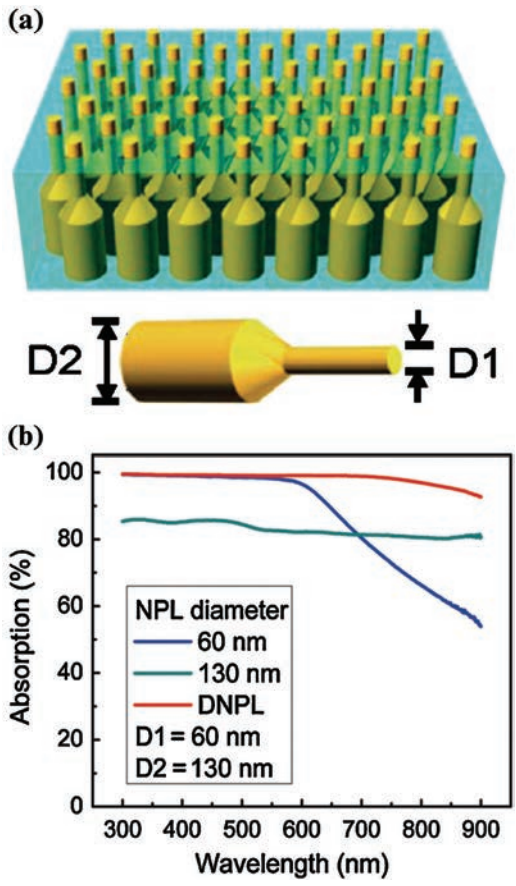

Figure 1. (a) Schematic diagram of the dual-diameter nanopillar array layer (DNPL); and (b) light absorbance comparison of the DNPL layer with those of uniform diameter nanopillar arrays. Reprinted with permission from Fan *et al*. (2010).

NWs (~1 cm^2/Vs) is 1–2 orders of magnitude faster than those in polycrystalline (Feng *et al.*, 2008), which is even higher in the case of single-crystalline ZnO NWs (1–5 cm^2/Vs; Law *et al.*, 2005). At the same time, the first-principle calculation also revealed that the injection time of excited electrons are 50 fs (femtosecond), and thus the recombination of electron and hole is negligible (Meng *et al.*, 2008). However, if the 1D TiO_2 materials are polycrystalline, then the collection time (mobility) is comparable with that of zero-dimensional (0D) nanomaterials as the electron transport is determined by the capture and release process by the surface traps (Enache-Pommer *et al.*, 2007; Zhu *et al.*, 2007). The recombination time in 1D TiO_2 materials is much longer than that in 0D materials. It is because the recombination centers might be distributed differently on the surface of 0D and 1D nanomaterials. Also, the radial electric field might be existed in 1D nanowires which prevents the carriers recombination (especially when there is a hetero-structure, as shown in Figure 7a). This way, the longer recombination time might account for the enhanced electron collection efficiency in 1D TiO_2 nanomaterials (Enache-Pommer *et al.* 2007; Gubbala *et al.* 2008; Law *et al.* 2006).

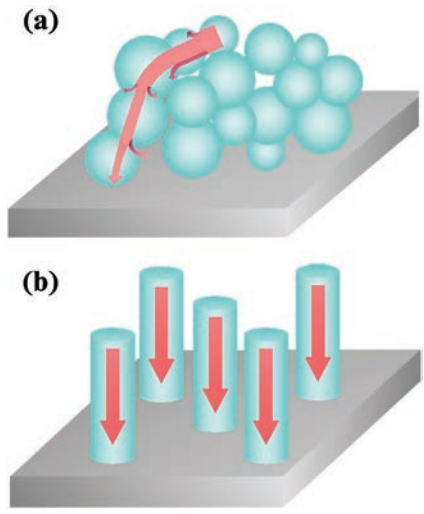

Figure 2. Schematic comparison of electron pathways in (a) zero dimensional nanomaterials and (b) one-dimensional nanomaterials.

Besides, there are additional advantages of using 1D nanomaterials that are addressed here. For example, the mechanical property of 1D nanomaterials is also advantageous in the nanowire/nanoparticle composite solar cell structures, where mechanically induced cracks can be effectively prevented in the film (Tan and Wu, 2006), similar to the strengthening effect of steel bars in concretes. Moreover, due to the unique mechanical flexibility, 1D nanomaterials can be compatible with the flexible organic substrates, which can develop a hybrid approach to assemble nanomaterials on plastics to improve energy conversion efficiency while lowering the processing cost for flexible energy harvesting applications (Fan *et al.*, 2008, 2009a, 2009b, 2009c).

3. One-dimensional nanostructure-based PV devices

The PV device is usually a semiconductor diode, where the incident light is absorbed by the semiconductor with a bandgap smaller than the photon energy ($E_g < h\nu$). Once the absorbed photons generate pairs of electron and hole, these carriers will be separated by the internal electric field in the p–n junction, as shown in Figure 3a. In this process, photons with energy lower than the bandgap of active device materials will not be absorbed while the higher energy ones would create "hot carrier" dissipating more energy (Tisdale *et al.*, 2010), both of which will cause the photon energy loss resulting in a theoretical energy harvesting efficiency limit of 31% for the single-junction PVs, 43% for two-junction PVs and 66% for infinitely many junctions (Crabtree and Lewis, 2007; Lewis, 2007).

In order to understand the essence of 1D nanostructure-based PVs, fundamental studies of single NW PV device were performed. Typically, there are a variety of NW PV structures including the NW-metal Schottky contact structure (Kelzenberg *et al.*, 2008), NW

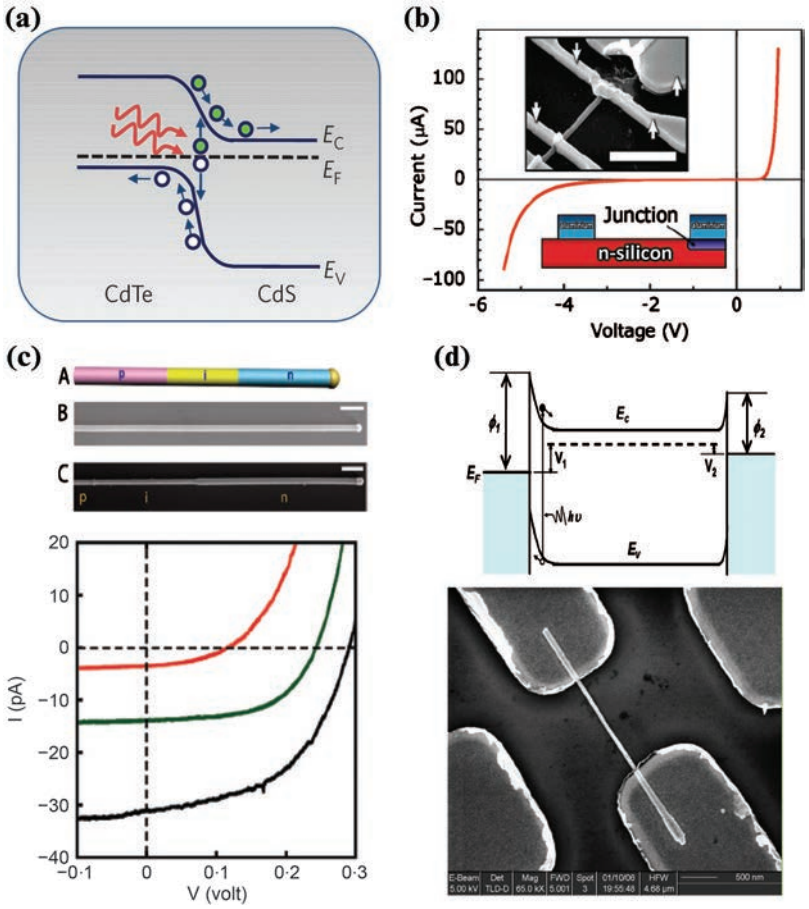

Figure 3. (a) Schematic view of the photovoltaic (PV) mechanism; (b) PVs based on metal-semiconductor Schottky contact; (c) PVs based on semiconductor p–n (p–i–n) junctions in single nanowire; and (d) PVs based on asymmetric contact. Reprinted with permission from Fan *et al.* (2009a, 2009b, 2009c), Kelzenberg *et al.* (2008), Kempa *et al.* (2008) and Liao *et al.* (2008).

axial p–n junction (Kempa *et al.*, 2008) and asymmetric junction configuration (Liao *et al.*, 2008), as shown in Figures 3(b)–3(d). Kelzenberg *et al.* (2008) prepared the single n-silicon NW with Schottky contact with aluminium electrode-doped p-silicon region, where this as-synthesised PV cell showed an energy conversion efficiency of 0.46%. By introducing an intrinsic layer into a silicon axial p–n junction to suppress the junction leakage, the open-circuit voltage (V_{oc}) and short-circuit current (I_{sc}) were increased from 0.12 V, 35 pA to 0.29 V, 31.1 pA, with a maximum efficiency of 0.5% (Kempa *et al.*, 2008). It is also noted that NWs with small diameters would favour the charge collection whereas large diameters would favour the higher open-circuit voltage; therefore, a compromised diameter of ~4 μm is expected considering the minority diffusion length of >2 μm in the experiment (Kelzenberg *et al.*, 2008). By inserting a dielectric layer on top of the NW surface, the light absorbance of the NW device was increased by 102% due to the off-resonance enhancement and resonance contribution (Liu *et al.*, 2011). However, the efficiency of single NW axial junction PV is still relatively low even though the voltage can be tuned by utilising the tandem structure (Heurlin *et al.*, 2011), because (a) low current density is a result of the small NW junction area and (b) the recombination of photo-carriers is induced by surface traps in the long axial transport process. Alternatively, radial junction PVs and three-dimensional (3D) PVs are actively explored to tackle these intrinsic problems.

To achieve the shorter carrier collection pathway, Tian *et al.* (2007) prepared the radial (coaxial) p–i–n junction silicon NW PV cell. The B-doped p-type core was prepared by chemical vapour deposition (CVD) method while P-doped n-type shell was deposited at higher temperature and lower pressure conditions. The silicon NWs were selectively etched by potassium hydroxide

solution as defined by lithography to expose the p-core, and metal contacts were then defined. This single NW radial junction PV cell showed a high energy conversion efficiency of 3.4% under 1 sun illumination. The polycrystalline n-type shell is helpful for the photon absorption, as well as for the carrier separation due to the negligible potential drop through the shell. Similarly, using an intrinsic $In_xGa_{1-x}N$ active layer for light absorption and junction leakage elimination, n-GaN/i-In_xGa_{1-x}N/p-GaN coaxial solar cells were prepared. This type of PV cell showed an extremely high V_{oc} (~1 V) and a relatively low I_{sc} (~58 pA), leading to an efficiency of only 0.19% (Dong *et al.*, 2009). Also, by introducing an intrinsic layer between silicon-doped p-GaAs core and silicon-doped n-GaAs shell (different growth conditions lead to different doping effects of silicon in gallium arsenide (GaAs) NWs by substituting Ga or As sublattice position), the highest single NW PV cell efficiency of 4.5% was obtained, as shown in Figure 4 (Colombo *et al.*, 2009). All these have demonstrated the potential of radial NW junction configuration for high-performance solar cells.

Apart from the single NW PV structure, for practical applications, silicon NW arrays prepared by CVD or wet chemical etching methods are thoroughly studied (Garnett and Yang, 2008; Tsakalakos *et al.*, 2007; Peng and Lee, 2011; Peng *et al.*, 2005). Compared with the single NW configuration, the short-circuit current is expected to increase due to the larger junction area and better light absorbance. Peng *et al.* (2005) prepared n-silicon NW arrays by wet chemical etching method on the n-silicon substrate, and then converted the NW arrays to p-type by the thermal phosphorus diffusion method. The as-obtained axial p–n junction arrays showed a respectable efficiency of 9.31% on single-crystalline silicon substrates and 4.73% on polycrystalline substrates. The authors analysed that there might be some efficiency loss due to the carrier recombination in the surface traps of NWs. However, the efficiency was not improved by using the radial junction configuration (0.5%) because of the high series resistance and significant interfacial recombination requiring the surface passivation (Garnett and Yang, 2008).

Similarly, III–V compound semiconductor NW arrays were also prepared for PVs, such as p-type magnesium-doped gallium nitride NW array on n-type Si(111) (efficiency =2.73%; Tang *et al.*, 2008), indium phosphate core–shell NW array (3.37%; Goto *et al.*, 2009) and tellurium-doped n-GaAs/Be-doped p-GaAs core–shell NW array (0.83%; Czaban *et al.*, 2009). Even though compound semiconductors usually have a better light absorbance than silicon, the relatively low efficiency here infers a large portion of the energy loss due to surface recombination. PV devices based on the II–VI compound semiconductor Cu_2O–ZnO p–n junction was first introduced by Yuhas and Yang (2009) with a low efficiency of 0.053% and recently improved to 0.5% (Musselman *et al.*, 2010). Fan *et al.* prepared the 3D p–n junction formed by embedding polycrystalline p-CdTe on n-CdS nanopillar array and a high efficiency of ~6% was obtained under 1.5 AM illumination as shown in Figure 5, with the potential to a further increase by

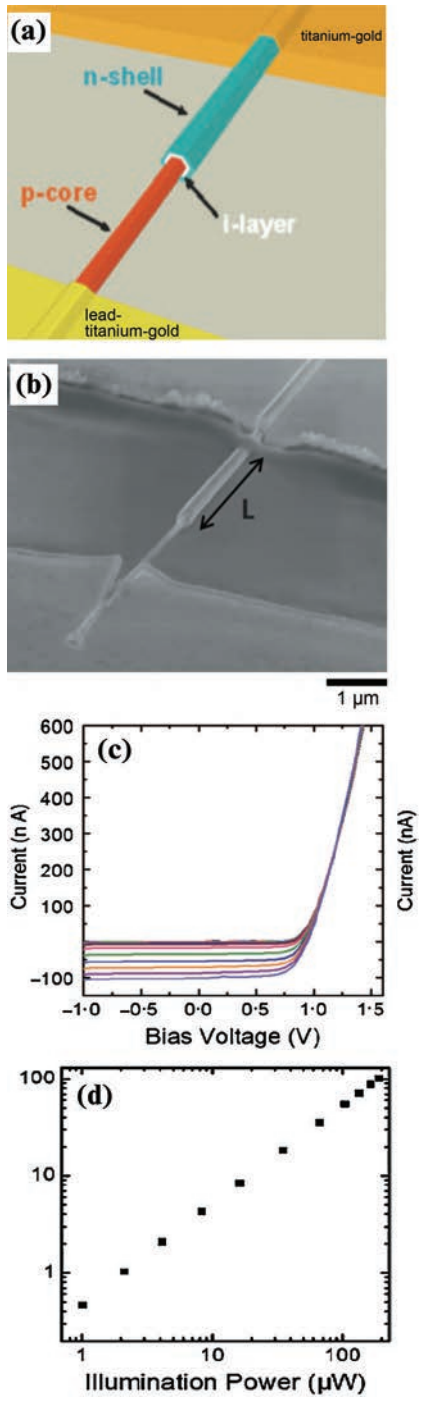

Figure 4. (a) Schematic view of the p–i–n structured GaAs nanowires radial photovoltaic (PV); (b) scanning electron microscope image of the corresponding PV structure; (c, d) I–V characteristics of GaAs radial PV cell under different illumination intensities from 1–200 μW. Reprinted with permission from Colombo *et al.* (2009).

optimising the top contact and using anti-reflection layers (Fan and Ho, 2011; Fan *et al.*, 2009a, 2009b, 2009c). Due to the low surface

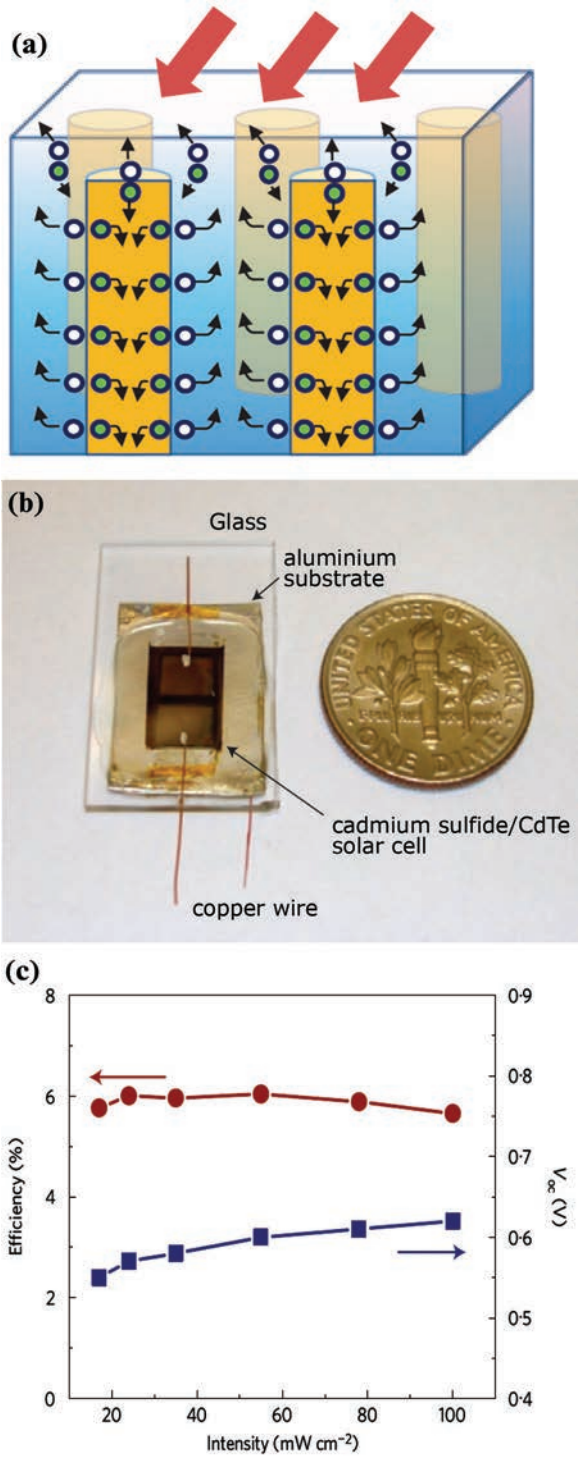

Figure 5. (a) Schematic view of the three-dimensional (3D) p-CdTe-n-CdS junction photovoltaic (PV); (b) an optical image of a fully fabricated 3D cell bonded on a glass substrate; and (c) energy conversion efficiency and open-circuit voltage of this PV structure under different illumination intensities. Reprinted with permission from Fan *et al.* (2009a, 2009b, 2009c).

recombination velocity of the carriers, this kind of II–VI compound material system is promising for the highly efficient future PVs (Kapadia *et al.*, 2010).

4. One-dimensional nanostructure-based PECs

In addition to the PV cells, PECs are another kind of device for solar energy harvesting (Gratzel, 2001). To date, there are mainly two kinds of PECs: DSSCs (Gratzel, 2005) and quantum dot-sensitised solar cells (QDSSCs; Kamat, 2008). The major difference between these two cells lies in the different materials used for light absorption, where photosensitive dyes are utilised in DSSCs and small bandgap semiconductor quantum dots are used in QDSSCs (Hotchandani and Kamat, 1992; Seabold *et al.*, 2008; Tak *et al.*, 2009). In both cases, 1D nanomaterials show their potential as active materials due to their unique light-scattering effect and electron transport expressway. In this review, the 1D nanomaterial-based anode in DSSCs is discussed in detail.

In 1988–1991, Gratzel's group first reported the DSSCs based on the low-cost TiO_2 nanoparticles instead of the expensive single-crystalline silicon cells in order to reduce the cost (Oregan and Gratzel, 1991; Vlachopoulos *et al.*, 1988). In this device, photons are absorbed by the sensitive dye to produce excitons and electrons are then swept and collected in the TiO_2 anode. For the compensation of electrons, I_3^-/I^- reduction/oxidation pair is used to transfer the outcircuit electrons from the conductive cathode to the excited dyes, as shown in Figure 6. This working principle is different from PVs where the light absorption and photoexcited electron collection take place in the same semiconductor material. One obvious advantage of this two-step process in DSSCs is the usage of dyes as more effective light absorbers, which have higher light absorption efficiency due to larger overlap with the sunlight spectra than the large bandgap semiconductors. In this case, the role of nanomaterials is to serve as an electron pathway for the excitons collection, which should be stable in electrolyte solutions (Gratzel, 2001). DSSCs have a high solar-to-electricity yield of ~8% in their initial stages, which has further increased to ~11% at present (Gratzel, 2005). Here, utilising 1D nanomaterials is fairly fascinating in making such practical applications feasible for the low-cost structure and potentially improved efficiency.

The incident photon-to-current conversion efficiency (IPCE) is defined as

$$\mathrm{IPCE} = \mathrm{LHE} \cdot \varphi_{\mathrm{injection}} \cdot \eta_{\mathrm{collection}}$$

where LHE is the light harvesting efficiency, $\varphi_{\mathrm{injection}}$ is the electron injection efficiency from the excited dye molecule to conduction band of the TiO_2 and $\eta_{\mathrm{collection}}$ is the electron collection efficiency. Apart from the well-chosen dyes with absorption spectra having the largest overlap with the solar incident spectra (Meng *et al.*, 2008; Wang *et al.*, 2007), 1D material can scatter more light

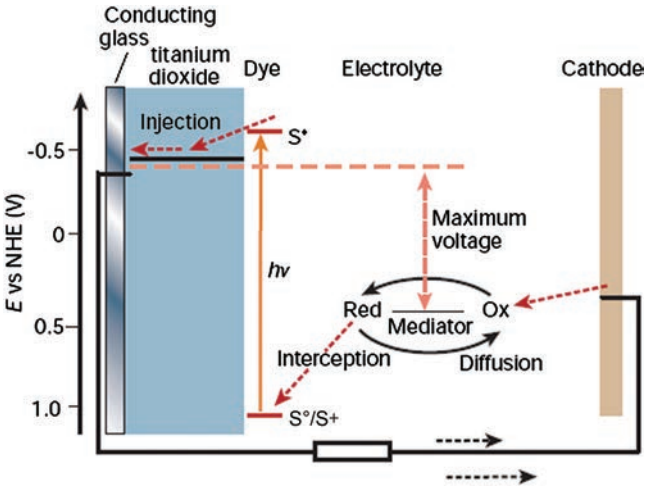

Figure 6. Mechanism of dye-sensitised solar cells. The titanium oxide photoanode receives electrons from photoexcited dyes. The positively charged dyes are then reduced by a mediator redox pair dissolved in the electrolyte. The mediator redox pair is then regenerated by reduction near the cathode by the electrons. Reprinted with permission from Gratzel (2001).

for further absorption by the dyes and thus the LHE can be subsequently improved. However, one bottleneck in the efficiency enhancement is the large carrier diffusion length in particulate TiO_2 anode; therefore, the recombination of electrons and holes competes with the electron accumulation into the anode, resulting in the low $\eta_{collection}$. To achieve high charge separation efficiency, the charge injection velocity into anode should be at least 100 times faster than the recombination velocity (Gratzel, 2005). Fortunately, 1D TiO_2 nanorods or nanotubes serve a direct pathway of photoelectrons into the anode so that the separation of electrons and holes is more effective (Enache-Pommer *et al.*, 2007; Mor *et al.*, 2006). For example, the recombination time is 150 times larger than the injection time, leading to a near 100% photoelectron collection efficiency (Enache-Pommer *et al.*, 2007). Besides, the overall resistance of the cell would be reduced because of the lower resistance "electron expressway"; as a result, the corresponding filling factor of the cell would also be increased (Jiu *et al.*, 2006).

Moreover, the electron collection time can be further reduced by introducing another semiconductor shell with the well-aligned band energy in order to improve the efficiency (Gubbala *et al.*, 2008; Law *et al.*, 2006). The conduction band potential of the shell should be lower than that of the core wire, which favours electron injection into the core and helps reducing electron recombination by the introduced potential gradient. For example, there is an energy barrier of 75–150 meV between the ZnO core and TiO_2 shell, which helps to inhibit electron/hole recombination at the surface, as shown in Figure 7 (Law *et al.*, 2006). In this core–shell structured photoanode, the physical dimension or its distribution

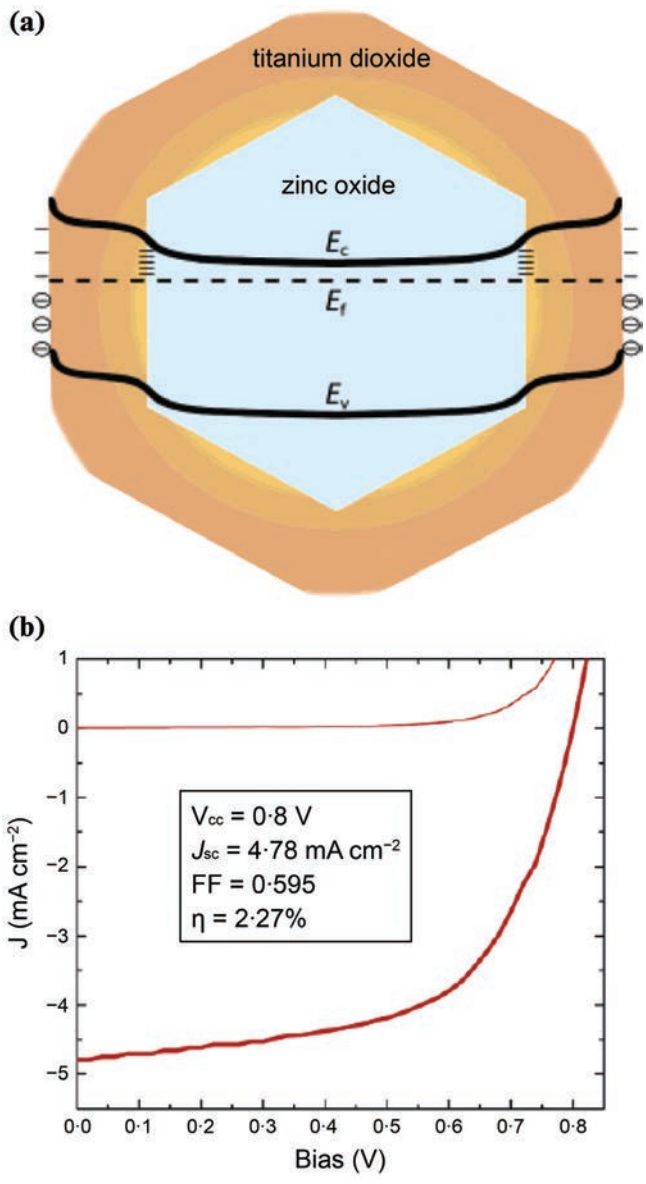

Figure 7. (a) Schematic energy level of zinc oxide (ZnO) core and titanium oxide (TiO_2) shell; and (b) I–V characteristics of PV cell based on ZnO–TiO_2 core–shell structure. Reprinted with permission from Law *et al.* (2006).

of the decorating shell should be well designed to achieve a high-performance cell (Kongkanand *et al.*, 2008; Zhang *et al.*, 2008). It is also noted that special care should be taken to control the crystal phase when preparing these 1D nanomaterials in order to have enhanced electron collection efficiency. For example, TiO_2-B NWs illustrated the worst performance compared with TiO_2-B nanoparticles due to improper energy band alignment and slower electron mobility (Qi *et al.*, 2010) whereas anatase and rutile phase TiO_2 1D nanomaterials showed an enhanced cell performance.

However, the anode completely based on 1D materials cannot yield enhanced efficiency because of the relatively lower dye load which is a result of smaller surface area than nanoparticles, except for the double-surfaced nanotubes, which can have comparable surface areas with nanoparticles (Bang and Kamat, 2010; Baxter and Aydil, 2005; Hafez *et al.*, 2010; Gubbala *et al.*, 2008; Law *et al.*, 2006; Martinson *et al.*, 2007; Zhu *et al.*, 2007). In fact, the highest efficiency of DSSCs based on 1D TiO_2 alone as the anode material is 7.29% with TiO_2 nanorod structures (Jiu *et al.*, 2006); because the nanorods have a length of 100–300 nm and a diameter of 20–30 nm, and these affect their total surface area to a certain extent. Nevertheless, the achieved efficiency here is still lower than one of the best TiO_2 nanoparticle-based DSSC (~8%; Feng *et al.*, 2008). Consequently, newer generation cells have been assembled to hierarchical structures or combined with 0D particles to form the hybrid anode to improve the efficiency (Fujihara *et al.*, 2007; Jiang *et al.*, 2007; Wang *et al.*, 2009). For example, as demonstrated in Figure 8, Tan and Wu (2006) found that 20 wt% (weight percent) TiO_2 nanotubes loaded on TiO_2 nanoparticles resulted in a higher efficiency of 8.6% as compared with 6.7% efficiency of pure nanoparticles. Suzuki *et al.* (2006) also found a similar improvement in the cell efficiency with the best load of 5–10 wt% nanowires. However, further increase in the percentage of TiO_2 nanowires will eventually decrease the efficiency due to the relatively lower surface area.

Another recent development is the adoption of high electron mobility semiconductor NWs such as ZnO (Law *et al.*, 2005), stannic oxide (Gubbala *et al.*, 2008) and gallium nitride (Chen *et al.*, 2010) with TiO_2 materials in the anode. Stannic oxide (Gubbala *et al.*, 2008) and gallium nitride NWs (Chen *et al.*, 2010) have high electron mobility and stability in the electrolyte solution; therefore, they are promising for anode components in DSSCs. Chen *et al.* (2010) also found that the gallium nitride NW surface should be modified with TiO_2 shell for good coherent with dyes as gallium nitride is too inert to get good adhesion with dye molecules. Just with this surface modification, the resulting cell efficiency increased much from 0.003% to 0.44% for the non-optimised cell structure. Until recently, silicon NW arrays prepared by vapour–liquid–solid growth using copper as the catalyst showed improved efficiency up to 3% (Boettcher *et al.*, 2010). Although the efficiency of DSSCs is still low compared with one of the conventional PV cells, all recent developments in DSSCs, especially the application of 1D nanomaterials in the anode, have shown the potential for the low-cost and efficient energy harvesting devices for the future.

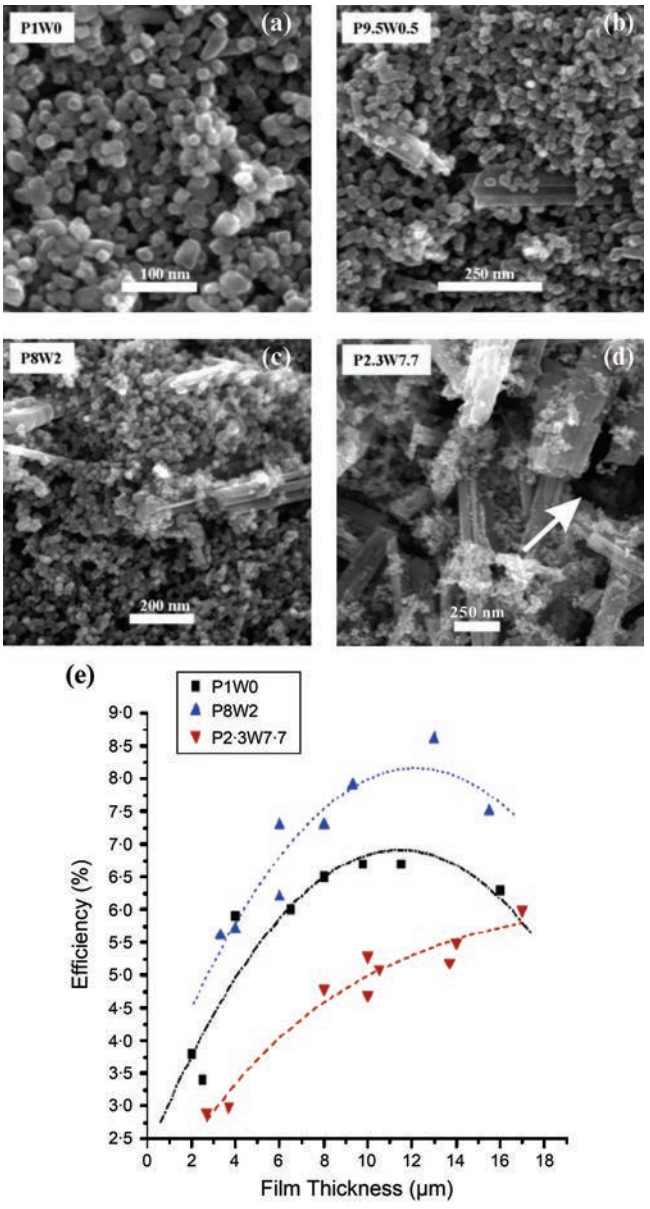

Figure 8. Cross section scanning electron images of (a) titanium oxide (TiO_2) nanoparticles anode (P1W0); (b) hybrid anode with TiO_2 nanowire (NW) load 5% (P9.5W0.5); (c) hybrid anode with TiO_2 NW load 20% (P8W2), (d) hybrid anode with TiO_2 NW load 77% (P2.3W7.7); and (e) thickness dependence of the energy conversion efficiencies of the photoanodes under AM 1.5 G sunlight. The anode with TiO_2 NWs loaded at 20% (P8W2) has the highest solar energy harvesting efficiency. Reprinted with permission from Tan and Wu (2006).

5. One-dimensional nanostructure-based solar hydrogen production

One of the main problems in utilising PVs and PECs for the generation of energy is their dependence on the geographical location and operational time span, which calls into the question of energy storage. Typically, the energy generated is stored as electricity in the batteries but the storage cannot persist for a long duration with a moderate efficiency. In contrast, hydrogen is believed to be one of the best choices to store the electrical energy in the form of chemical bonds with a higher efficiency and longer storage time, which is also an alternative to liquid fuels and has relatively clean combustion (Bolton, 1978; Maugh, 1982). Although PVs and PECs

can be combined with water electrolysis cell to produce hydrogen, the cost is relatively high and the efficiency loss is also significant in this two-step process. On the other hand, hydrogen can also be produced in situ in the photochemical cells by using photosensitive anode and/or cathode with help of electrolytes such as acid or alkaline, as shown in Figure 9 (Fujishima and Honda, 1972; Gratzel, 2001; Heller, 1984). Taking the photosensitive anode as an example, holes produced in the metal oxide semiconductor would diffuse into the interface with water, where water would be oxidised into oxygen. Furthermore, electrons would be injected to the back contact due to the lower Fermi level of the metal, and subsequently be transported to the cathode to reduce water into hydrogen with the help of the catalysts (Gratzel, 2001; Heller, 1984). Hydrogen can be produced from solar energy harvesting using this method.

In this process, there are many barriers that should be surmounted to achieve a high solar-to-hydrogen conversion efficiency, including (a) bandgap engineering for the enhanced photon absorption with better overlap with the solar spectra; (b) suppression of the photogenerated excitons recombination and (c) elimination of the reverse reaction of the solar-harvested hydrogen with surrounding oxygen to form water (Bak *et al.*, 2002; Ni *et al.*, 2007). As one of the unique characteristics of this cell is to utilise the photosensitive electrode, made of cost-effective polycrystalline metal oxide semiconductor particles, similar to the ones in DSSCs, this kind of cells also face the same problems because of (a) significant reflection of the incident light and (b) electron/hole recombination in the photosensitive anode and/or cathode. Again, using 1D nanostructured materials, the recombination loss of electrons is highly suppressed and the photon absorption is greatly enhanced by the internal scattering among the nanostructures. The use of TiO_2 and ZnO semiconductor materials as anode in the solar hydrogen production is well summarised elsewhere (Van de Krol *et al.*, 2008; Li and Zhang, 2010; Shankar *et al.*, 2009). It is noticeable that even though a high efficiency of 16.25% (efficiency at certain wavelength range) was gained in the ultraviolet (UV) range of 320–400 nm by using 45-μm TiO_2 nanotubes under 100 mW/cm^2 illumination (Paulose *et al.*, 2006), the overall solar-to-electricity conversion is relatively low considering the small fraction (~5%) of the UV light energy in the solar energy.

Notably, similar to DSSCs, 1D nanomaterials in the anode can also be integrated with other materials for higher efficiency (Jin *et al.*, 2007; Wang *et al.*, 2010; Yang *et al.*, 2009). For example, 3.7% nitrogen-doped ZnO nanorods showed an increased IPCE compared with pure ZnO nanorods (Yang *et al.*, 2009), but the effective absorption range is below 400 nm in the wavelength. The low IPCE in >400-nm wavelength leads to a low conversion efficiency of ~0.15%. Moreover, double side ZnO nanorod arrays on indium tin oxide glass was decorated with cadmium sulfide on one side and cadmium selenide on the other side for effective light absorption, and a high IPCE (45%) was gained in the wavelength range of 300–600 nm, as shown in Figure 10 (Wang *et al.*, 2010).

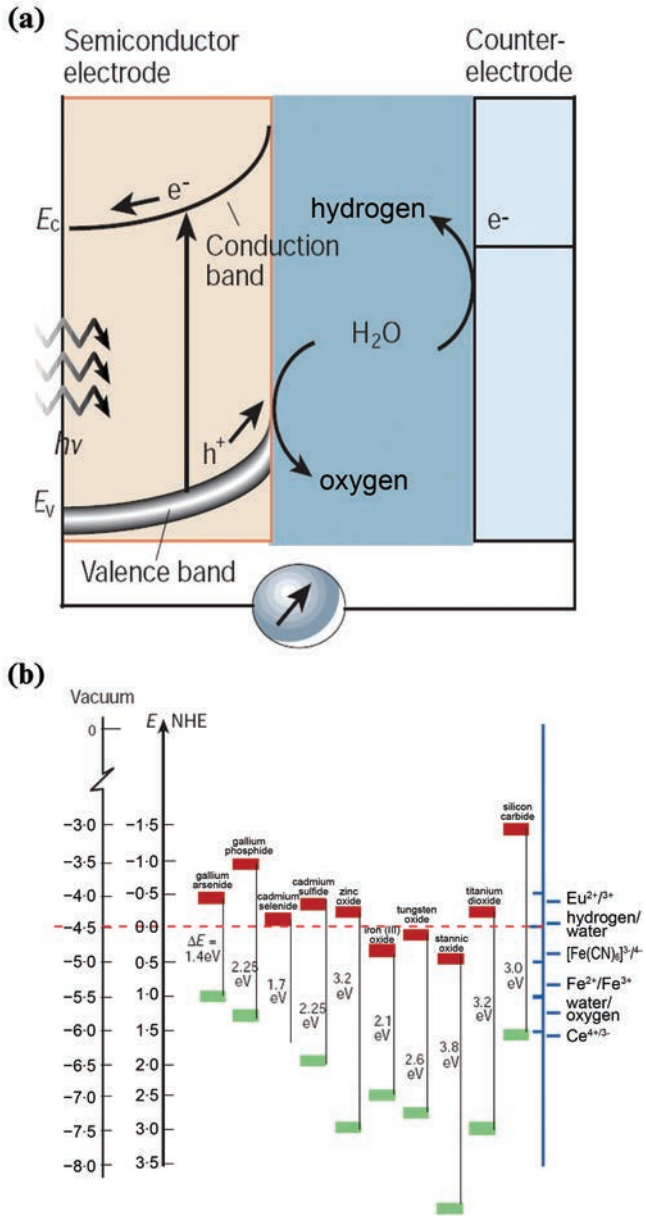

Figure 9. (a) Separation, transport and reaction of photogenerated electron–hole pairs in photoanode; (b) band positions of several semiconductors in contact with aqueous electrolyte at pH 1, and the standard potentials of several redox couples against standard hydrogen electrode potential. Theoretically, photoexcited electrons with energy higher than the hydrogen/water potential will reduce water to hydrogen, and photoexcited holes with energy lower than the water/oxygen potential will oxidise water to oxygen. Reprinted with permission from Gratzel (2001).

Although TiO_2, ZnO and strontium titanate are widely used for photosensitive anode in the solar hydrogen production due to their stability in the electrolyte and suitable band positions

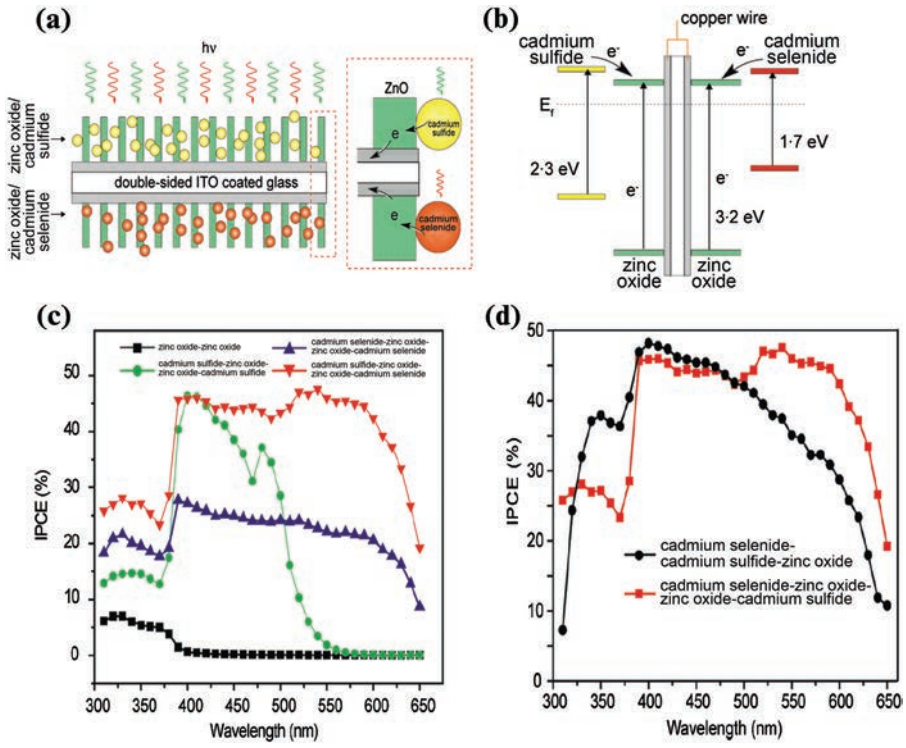

Figure 10. (a) Schematic view of the double-sided CdS–ZnO–ZnO–CdSe photoanode; (b) band energy alignment of the double-sided photoanode; (c) incident photon-to-current conversion efficiency (IPCE) spectra of the doubled-sided photoanode in the range of 310–650 nm at 0 V; and (d) IPCE comparison with single-sided CdSe–CdS–ZnO photoanode. Reprinted with permission from Wang *et al.* (2010).

for water splitting, the relatively large bandgap inhibits further enhancement in the their efficiency (Khaselev and Turner, 1998). In this context, 1D nanomaterials with the smaller bandgap such as ferrous oxide (1.9–2.1 eV; Vayssieres *et al.*, 2005), CuO/Cu_2O (1.2–1.9 eV; Barreca *et al.*, 2009; Siripala *et al.*, 2003; Zhao *et al.*, 2010), tungsten nitride (2.2 eV; Chakrapani *et al.*, 2009) as well as other III–V and II–VI compound semiconductors are attractive for the anode materials here (Aryal *et al.*, 2010; Hensel *et al.*, 2010; Yu *et al.*, 2005). For example, branched copper oxide NW arrays showed a solar-to-hydrogen conversion efficiency of 0.6% (Barreca *et al.*, 2009) whereas using CuO/ZnO core–shell nanorod arrays, the solar-to-current conversion efficiency was as high as 0.71% due to the anti-reflection role of the nanorod array and the wider absorbance spectra as well as better carrier separation and the collection property of p–n junction (Zhao *et al.*, 2010). But the issue of band position should be carefully considered as an external bias should be applied if the conduction band position is lower than the H^+/hydrogen potential or the valence band position is higher than the OH^-/oxygen potential (Van de Krol *et al.*, 2008; Zhao *et al.* 2010). Besides, the stability is also a concern, which might necessitate the combination with other anti-corrosive materials in eletrolyte solutions (Hwang *et al.*, 2009; Nowotny *et al.*, 2005; Siripala *et al.*, 2003).

6. Conclusion

In summary, 1D nanomaterials are versatile in photon absorption and carrier separation/collection due to their large ratio and anisotropic properties, which could enhance the solar energy harvesting efficiencies. Tailoring the 1D nanomaterials into hierarchical structures or hybrid structures with supplementary materials – for example core–shell structure, 0D and 1D hybrid materials – can further increase the light absorbance and/or improve the carrier collection efficiency. Therefore, by using bandgap engineering and nanostructure design, 1D nanomaterials hold the potential for the cost effective and high efficiency PV and PEC solar cells. However, due to the strict confinement of band energy alignment with the water-splitting potential and the stability in electrolyte solutions, there is still a huge urge to explore more 1D nanomaterial design and fabrication to further increase the solar hydrogen production efficiency.

Acknowledgements

This work was financially supported by the City University of Hong Kong (Project No. 7200203 & 7002597) and by the General Research Fund of the Research Grants Council of Hong Kong SAR, China, under Project no. CityU 101210.

REFERENCES

Aryal K, Pantha BN, Li J, Lin JY and Jiang HX (2010) Hydrogen generation by solar water splitting using p-InGaN photoelectrochemical cells. *Applied Physics Letters* **96(5)**: 052110.

Bak T, Nowotny J, Rekas M and Sorrell CC (2002) Photo-electrochemical hydrogen generation from water using solar energy. Materials-related aspects. *International Journal of Hydrogen Energy* **27(10)**: 991–1022.

Bang JH and Kamat PV (2010) Solar cells by design: Photoelectrochemistry of TiO_2 nanorod arrays decorated with CdSe. *Advanced Functional Materials* **20(12)**: 1970–1976.

Barreca D, Fornasiero P, Gasparotto A *et al.* (2009) The potential of supported Cu_2O and CuO nanosystems in photocatalytic H_2 production. *Chemsuschem* **2(3)**: 230–233.

Baxter JB and Aydil ES (2005) Nanowire-based dye-sensitized solar cells. *Applied Physics Letters* **86(5)**: 053114.

Boettcher SW, Spurgeon JM, Putnam MC *et al.* (2010) Energy-conversion properties of vapor–liquid–solid-grown silicon wire-array photocathodes. *Science* **327(5962)**: 185–187.

Bolton JR (1978) Solar fuels. *Science* **202(4369)**: 705–711.

Chakrapani V, Thangala J and Sunkara MK (2009) WO_3 and W_2N nanowire arrays for photoelectrochemical hydrogen production. *International Journal of Hydrogen Energy* **34(22)**: 9050–9059.

Chen XY, Yip CT, Fung MK, Djurisic AB and Chan WK (2010) GaN-nanowire-based dye-sensitized solar cells. *Applied Physics a-Materials Science & Processing* **100(1)**: 15–19.

Cole T (1983) Thermoelectric energy-conversion with solid electrolytes. *Science* **221(4614)**: 915–920.

Colombo C, Heiss M, Gratzel M and Morral AFI (2009) Gallium arsenide p–i–n radial structures for photovoltaic applications. *Applied Physics Letters* **94(17)**: 173108.

Crabtree GW and Lewis NS (2007) Solar energy conversion. *Physics Today* **60(3)**: 37–42.

Czaban JA, Thompson DA and LaPierre RR (2009) GaAs core-shell nanowires for photovoltaic applications. *Nano Letters* **9(1)**: 148–154.

Diedenhofen SL, Vecchi G, Algra RE *et al.*, (2009) Broad-band and omnidirectional antireflection coatings based on semiconductor nanorods. *Advanced Materials* **21(9)**: 973–978.

Dong YJ, Tian BZ, Kempa TJ and Lieber CM (2009) Coaxial group III-nitride nanowire photovoltaics. *Nano Letters* **9(5)**: 2183–2187.

Enache-Pommer E, Boercker JE and Aydil ES (2007) Electron transport and recombination in polycrystalline TiO_2 nanowire dye-sensitized solar cells. *Applied Physics Letters* **91(12)**: 123116.

Fan Z and Ho JC (2011) Self-assembly of one-dimensional nanomaterials for cost-effective photovoltaics. *International Journal of Nanoparticles* **4(2)**: 164–183.

Fan ZY, Ho JC, Jacobson ZA, Yerushalmi R, Alley RL, Razavi H and Javey A (2008) Wafer-scale assembly of highly ordered semiconductor nanowire arrays by contact printing. *Nano Letters* **8(1)**: 20–25.

Fan ZY, Ho JC, Takahashi T, Yerushalmi R, Takei K, *et al.* (2009a) Toward the development of printable nanowire electronics and sensors. *Advanced Materials* **21(37)**: 3730–3743.

Fan ZY, Razavi H, Do JW *et al.* (2009b) Three-dimensional nanopillar-array photovoltaics on low-cost and flexible substrates. *Nature Materials* **8(8)**: 648–653.

Fan ZY, Ruebusch DJ, Rathore AA *et al.* (2009c) Challenges and prospects of nanopillar-based solar cells. *Nano Research* **2(11)**: 829–843.

Fan ZY, Kapadia R, Leu PW *et al.* (2010) Ordered arrays of dual-diameter nanopillars for maximized optical absorption. *Nano Letters* **10(10):** 3823–3827.

Feng XJ, Shankar K, Varghese OK *et al.* (2008) Vertically aligned single crystal TiO_2 nanowire arrays grown directly on transparent conducting oxide coated glass: Synthesis details and applications. *Nano Letters* **8(11)**: 3781–3786.

Ford AC, Ho JC, Chueh YL *et al.* (2009) Diameter-dependent electron mobility of InAs nanowires. *Nano Letters* **9(1)**: 360–365.

Fujihara K, Kumar A, Jose R, Ramakrishna S and Uchida S (2007) Spray deposition of electrospun TiO_2 nanorods for dye-sensitized solar cell. *Nanotechnology* **18(36)**: 365709.

Fujishima A and Honda K (1972) Electrochemical photolysis of water at a semiconductor electrode. *Nature* **238(5358)**: 37–38.

Garnett EC and Yang PD (2008) Silicon nanowire radial p–n junction solar cells. *Journal of the American Chemical Society* **130(29)**: 9224–9225.

Garnett E and Yang PD (2010) Light trapping in silicon nanowire solar cells. *Nano Letters* **10(3)**: 1082–1087.

Garnett E, Brongersma M, Cui Y and McGehee M (2011) Nanowire Solar Cells. *Annual Review of Materials Research* **41(1)**: 269–295.

Gratzel M (2001) Photoelectrochemical cells. *Nature* **414(6861)**: 338–344.

Gratzel M (2005) Solar energy conversion by dye-sensitized photovoltaic cells. *Inorganic Chemistry* **44(20)**: 6841–6851.

Goto H, Nosaki K, Tomioka K, Hara S, Hiruma K, Motohisa J and Fukui T (2009) Growth of core-shell InP nanowires for photovoltaic application by selective-area metal organic vapor phase epitaxy. *Applied Physics Express* **2(3)**: 035004.

Gubbala S, Chakrapani V, Kumar V and Sunkara MK (2008) Band-edge engineered hybrid structures for dye-sensitized solar cells based on SnO_2 nanowires. *Advanced Functional Materials* **18(16)**: 2411–2418.

Gudiksen MS, Lauhon LJ, Wang J, Smith DC and Lieber CM (2002) Growth of nanowire superlattice structures for nanoscale photonics and electronics. *Nature* **415(6872)**: 617–620.

Hafez H, Lan Z, Li Q and Wu J (2010) High efficiency dye-sensitized solar cell based on novel TiO_2 nanorod/nanoparticle bilayer electrode. *Nanotechnology, Science and Applications* **3**: 45–51.

Heller A (1984) Hydrogen-evolving solar-cells. *Science* **223(4641)**: 1141–1148.

Hensel J, Wang G, Li Y and Zhang JZ (2010) Synergistic effect of CdSe quantum dot sensitization and nitrogen doping of TiO_2 nanostructures for photoelectrochemical solar hydrogen generation. *Nano Letters* **10(2)**: 478–483.

Heurlin M, Wickert P, Falt S *et al.* (2011) Axial InP nanowire tandem junction grown on a silicon substrate. *Nano Letters* **11(5)**: 2028–2031.

Hochbaum AI and Yang PD (2010) Semiconductor nanowires for energy conversion. *Chemical Reviews* **110(1):** 527–546.

Hotchandani S and Kamat PV (1992) Charge-transfer processes in coupled semiconductor systems – photochemistry and photoelectrochemistry of the colloidal CdS–ZnO system. *Journal of Physical Chemistry* **96(16)**: 6834–6839.

Hu L and Chen G (2007) Analysis of optical absorption in silicon nanowire arrays for photovoltaic applications. *Nano Letters* **7(11)**: 3249–3252.

Huynh WU, Dittmer JJ and Alivisatos AP (2002) Hybrid nanorod-polymer solar cells. *Science* **295(5564)**: 2425–2427.

Hwang YJ, Boukai A and Yang PD (2009) High density n-Si/n-TiO_2 core/shell nanowire arrays with enhanced photoactivity. *Nano Letters* **9(1)**: 410–415.

Jiang CY, Sun XW, Lo GQ, Kwong DL and Wang JX (2007) Improved dye-sensitized solar cells with a ZnO-nanoflower photoanode. *Applied Physics Letters* **90(26)**: 263501.

Jin Z, Zhang X, Li Y, Li S and Lu G (2007) 5.1% Apparent quantum efficiency for stable hydrogen generation over eosin-sensitized CuO/TiO_2 photocatalyst under visible light irradiation. *Catalysis Communications* **8(8)**: 1267–1273.

Jiu JT, Isoda S, Wang FM and Adachi M (2006) Dye-sensitized solar cells based on a single-crystalline TiO_2 nanorod film. *Journal of Physical Chemistry B* **110(5)**: 2087–2092.

Jung JY, Guo Z, Jee SW, Um HD, Park KT and Lee JH (2010) A strong antireflective solar cell prepared by tapering silicon nanowires. *Optics Express* **18(19)**: A286–A292.

Kamat PV (2007) Meeting the clean energy demand: Nanostructure architectures for solar energy conversion. *Journal of Physical Chemistry C* **111(7)**: 2834–2860.

Kamat PV (2008) Quantum dot solar cells. semiconductor nanocrystals as light harvesters. *Journal of Physical Chemistry C* **112(48)**: 18737–18753.

Kapadia R, Fan ZY and Javey A (2010) Design constraints and guidelines for CdS/CdTe nanopillar based photovoltaics. *Applied Physics Letters* **96(10)**: 103116.

Kelzenberg MD, Turner-Evans DB, Kayes BM *et al.* (2008) Photovoltaic measurements in single-nanowire silicon solar cells. *Nano Letters* **8(2)**: 710–714.

Kempa TJ, Tian BZ, Kim DR, Hu JS, Zheng XL and Lieber CM (2008) Single and tandem axial p–i–n nanowire photovoltaic devices. *Nano Letters* **8(10)**: 3456–3460.

Khaselev O and Turner JA (1998) A monolithic photovoltaic-photoelectrochemical device for hydrogen production via water splitting. *Science* **280(5362)**: 425–427.

Klimov VI (2006) Mechanisms for photogeneration and recombination of multiexcitons in semiconductor nanocrystals: Implications for lasing and solar energy conversion. *Journal of Physical Chemistry B* **110(34)**: 16827–16845.

Kongkanand A, Tvrdy K, Takechi K, Kuno M and Kamat PV (2008) Quantum dot solar cells. Tuning photoresponse through size and shape control of CdSe–TiO_2 architecture. *Journal of the American Chemical Society* **130(12)**: 4007–4015.

Law M, Greene LE, Johnson JC, Saykally R and Yang PD (2005) Nanowire dye-sensitized solar cells. *Nature Materials* **4(6)**: 455–459.

Law M, Greene LE, Radenovic A *et al.* (2006) ZnO–Al_2O_3 and ZnO–TiO_2 core-shell nanowire dye-sensitized solar cells. *Journal of Physical Chemistry B* **110(45)**: 22652–22663.

Lee YJ, Ruby DS, Peters DW, McKenzie BB and Hsu JWP (2008) ZnO nanostructures as efficient antireflection layers in solar cells. *Nano Letters* **8(5)**: 1501–1505.

Lewis NS (2007) Toward cost-effective solar energy use. *Science* **315(5813)**: 798–801.

Liao ZM, Xu J, Zhang JM and Yu DP (2008) Photovoltaic effect and charge storage in single ZnO nanowires. *Applied Physics Letters* **93(2)**: 023111.

Li Y and Zhang JZ (2010) Hydrogen generation from photoelectrochemical water splitting based on nanomaterials. *Laser & Photonics Reviews* **4(4)**: 517–528.

Liu WF, Oh JI and Shen WZ (2011) Light trapping in single coaxial nanowires for photovoltaic applications. *IEEE Electron Device Letters* **32(1)**: 45–47.

Martinson ABF, McGarrah JE, Parpia MOK and Hupp JT (2006) Dynamics of charge transport and recombination in ZnO nanorod array dye-sensitized solar cells. *Physical Chemistry Chemical Physics* **8(40)**: 4655–4659.

Martinson ABF, Elam JW, Hupp JT and Pellin MJ (2007) ZnO nanotube based dye-sensitized solar cells. *Nano Letters* **7(8)**: 2183–2187.

Maugh TH (1982) Two new routes to solar hydrogen. *Science* **218(4572)**: 557.

Meng S, Ren J and Kaxiras E (2008) Natural dyes adsorbed on TiO_2 nanowire for photovoltaic applications: Enhanced light absorption and ultrafast electron injection. *Nano Letters* **8(10)**: 3266–3272.

Mor GK, Shankar K, Paulose M, Varghese OK and Grimes CA (2006) Use of highly-ordered TiO_2 nanotube arrays in dye-sensitized solar cells. *Nano Letters* **6(2)**: 215–218.

Muskens OL, Rivas JG, Algra RE, Bakkers EPAM and Lagendijk A (2008) Design of light scattering in nanowire materials for photovoltaic applications. *Nano Letters* **8(9)**: 2638–2642.

Musselman KP, Wisnet A, Iza DC *et al.* (2010) Strong efficiency improvements in ultra-low-cost inorganic nanowire solar cells. *Advanced Materials* **22(35)**: E254–E258.

Ni M, Leung DYC, Sumathy K and Leung MKH (2007) A review and recent developments in photocatalytic water-splitting using TiO_2 for hydrogen production. *Renewable & Sustainable Energy Reviews* **11(3)**: 401–425.

Nowotny J, Sorrell CC, Bak T and Sheppard LR (2005) Solar-hydrogen: Unresolved problems in solid-state science. *Solar Energy* **78(5)**: 593–602.

Oregan B and Gratzel M (1991) A low-cost, high-efficiency solar-cell based on dye-sensitized colloidal TiO_2 films. *Nature* **353(6346)**: 737–740.

Paulose M, Shankar K, Yoriya S *et al.* (2006) Anodic growth of highly ordered TiO_2 nanotube arrays to 134 μm in length. *Journal of Physical Chemistry B* **110(33)**: 16179–16184.

Peng KQ and Lee ST (2011) Silicon nanowires for photovoltaic solar energy conversion. *Advanced Materials* **23(2)**: 198–215.

Peng KQ, Xu Y, Wu Y *et al.* (2005) Aligned single-crystalline Si nanowire arrays for photovoltaic applications. *Small* **1(11)**: 1062–1067.

Qi LH, Liu YJ and Li CY (2010) Controlled synthesis of TiO_2-B nanowires and nanoparticles for dye-sensitized solar cells. *Applied Surface Science* **257(5)**: 1660–1665.

Seabold JA, Shankar K, Wilke RHT *et al.* (2008) Photoelectrochemical properties of heterojunction CdTe/TiO_2 electrodes constructed using highly ordered TiO_2 nanotube arrays. *Chemistry of Materials* **20(16)**: 5266–5273.

Service RF (2005) Solar energy – Is it time to shoot for the Sun? *Science* **309(5734)**: 548–551.

Shankar K, Basham JI, Allam NK *et al.* (2009) Recent advances in the use of TiO_2 nanotube and nanowire arrays for oxidative photoelectrochemistry. *Journal of Physical Chemistry C* **113(16)**: 6327–6359.

Siripala W, Ivanovskaya A, Jaramillo TF, Baeck S-H and McFarland EW (2003) A Cu_2O/TiO_2 heterojunction thin film cathode for photoelectrocatalysis. *Solar Energy Materials and Solar Cells* **77(3)**: 229–237.

Suzuki Y, Ngamsinlapasathian S, Yoshida R and Yoshikawa S (2006) Partially nanowire-structured TiO_2 electrode for dye-sensitized solar cells. *Central European Journal of Chemistry* **4(3)**: 476–488.

Tan B and Wu YY (2006) Dye-sensitized solar cells based on anatase TiO_2 nanoparticle/nanowire composites. *Journal of Physical Chemistry B* **110(32)**: 15932–15938.

Tang YB, Chen ZH, Song HS *et al.* (2008) Vertically aligned p-type single-crystalline GaN nanorod arrays on n-type Si for heterojunction photovoltaic cells. *Nano Letters* **8(12)**: 4191–4195.

Tak Y, Hong SJ, Lee JS and Yong K (2009) Fabrication of ZnO/CdS core/shell nanowire arrays for efficient solar energy conversion. *Journal of Materials Chemistry* **19(33)**: 5945–5951.

Takei K, Takahashi T, Ho JC *et al.* (2010) Nanowire active-matrix circuitry for low-voltage macroscale artificial skin. *Nature Materials* **9(10)**: 821–826.

Tian BZ, Zheng XL, Kempa TJ *et al.* (2007) Coaxial silicon nanowires as solar cells and nanoelectronic power sources. *Nature* **449(7164)**: 885–890.

Tisdale WA, Williams KJ, Timp BA *et al.* (2010) Hot-electron transfer from semiconductor nanocrystals. *Science* **328(5985)**: 1543–1547.

Tsakalakos L, Balch J, Fronheiser J, Korevaar BA, Sulima O and Rand J (2007) Silicon nanowire solar cells. *Applied Physics Letters* **91(23)**: 233117.

Van de Krol R, Liang YQ and Schoonman J (2008) Solar hydrogen production with nanostructured metal oxides. *Journal of Materials Chemistry* **18(20)**: 2311–2320.

Vayssieres L, Sathe C, Butorin SM, Shuh DK, Nordgren J and Guo JH (2005) One-dimensional quantum-confinement effect in α-Fe_2O_3 ultrafine nanorod arrays. *Advanced Materials* **17(19)**: 2320–2323.

Vlachopoulos N, Liska P, Augustynski J and Gratzel M (1988) Very efficient visible-light energy harvesting and conversion by spectral sensitization of high surface-area polycrystalline titanium-dioxide films. *Journal of the American Chemical Society* **110(4)**: 1216–1220.

Wang DA, Hu TC, Hu LT, Yu B, Xia YQ, Zhou F and Liu WM (2009) Microstructured arrays of TiO_2 nanotubes for improved photo-electrocatalysis and mechanical stability. *Advanced Functional Materials* **19(12)**: 1930–1938.

Wang GM, Yang XY, Qian F, Zhang JZ and Li Y (2010) Double-sided CdS and CdSe quantum dot co-sensitized ZnO nanowire arrays for photoelectrochemical hydrogen generation. *Nano Letters* **10(3)**: 1088–1092.

Wang ZL and Song JH (2006) Piezoelectric nanogenerators based on zinc oxide nanowire arrays. *Science* **312(5771)**: 242–246.

Wang ZS, Kawauchi H, Kashima T and Arakawa H (2004) Significant influence of TiO_2 photoelectrode morphology on the energy conversion efficiency of N719 dye-sensitized solar cell. *Coordination Chemistry Reviews* **248(13–14)**: 1381–1389.

Wang ZS, Cui Y, Hara K, Dan-Oh Y, Kasada C and Shinpo A (2007) A high-light-harvesting-efficiency coumarin dye for stable dye-sensitized solar cells. *Advanced Materials* **19(8)**: 1138–1141.

Yan H, Choe HS, Nam S, Hu Y, Das S, Klemic JF, Ellenbogen JC and Lieber CM (2011) Programmable nanowire circuits for nanoprocessors. *Nature* **470(7333)**: 240–244.

Yan RX, Gargas D and Yang PD (2009) Nanowire photonics. *Nature Photonics* **3(10)**: 569–576.

Yang XY, Wolcott A, Wang GM, Sobo A, Fitzmorris RC, Qian F, Li Y and Zhang JZ (2009) Nitrogen-doped ZnO nanowire arrays

for photoelectrochemical water splitting. *Nano Letters* **9(6)**: 2331–2336.

Yu ZG, Pryor CE, Lau WH, Berding MA and MacQueen DB (2005) Core-shell nanorods for efficient photoelectrochemical hydrogen production. *Journal of Physical Chemistry B* **109(48)**: 22913–22919.

Yuhas BD and Yang PD (2009) Nanowire-based all-oxide solar cells. *Journal of the American Chemical Society* **131(10)**: 3756–3761.

Zhang QF, Chou TP, Russo B, Jenekhe SA and Cao G (2008) Polydisperse aggregates of ZnO nanocrystallites: A method for energy-conversion-efficiency enhancement in dye-sensitized solar cells. *Advanced Functional Materials* **18(11)**: 1654–1660.

Zhao X, Wang P and Li B (2010) CuO/ZnO core/shell heterostructure nanowire arrays: Synthesis, optical property, and energy application. *Chemical Communications* **46(36)**: 6768–6770.

Zhu K, Neale NR, Miedaner A and Frank AJ (2007) Enhanced charge-collection efficiencies and light scattering in dye-sensitized solar cells using oriented TiO_2 nanotubes arrays. *Nano Letters* **7(1)**: 69–74.

WHAT DO YOU THINK?

To discuss this paper, please email up to 500 words to the managing editor at nme@icepublishing.com

Your contribution will be forwarded to the author(s) for a reply and, if considered appropriate by the editor-in-chief, will be published as a discussion in a future issue of the journal.

ICE Science journals rely entirely on contributions sent in by professionals, academics and students coming from the field of materials science and engineering. Articles should be within 5000-7000 words long (short communications and opinion articles should be within 2000 words long), with adequate illustrations and references. To access our author guidelines and how to submit your paper, please refer to the journal website at www.icevirtuallibrary.com/nme